Detection of Nodules Showing Ground-Glass Opacity in the Lungs at Low-Dose Multidetector Computed Tomography: Phantom and Clinical Study

Yoshinori Funama, PhD, Kazuo Awai, MD,† Duo Liu, MD,† Seitaro Oda, MD,† Yumi Yanaga, MD,† Takeshi Nakaura, MD,† Koichi Kawanaka, MD,† Masamichi Shimamura, PhD,* and Yasuyuki Yamashita, MD†*

Objective: To investigate the effect of the radiation dose (tube current second product) and the attenuation value of nodules with ground-glass opacity (GGO) on their detectability at multidetector computed tomography (MDCT).

Methods: We scanned a chest CT phantom that included simulated GGO nodules with an MDCT scanner. The attenuation value of the simulated lung parenchyma was −900 Hounsfield units (HU); it was −800 and −650 HU for the simulated GGO nodules. We used a tube current second product of 180 mA as the standard and 21, 45, 60, and 90 mAs as the low-dose and performed receiver operating characteristic analysis to compare the performance of 5 radiologists in detecting GGO nodules at each milliampere. To assess the detectability of GGO nodules on human lung images, the observers were presented with 38 GGO nodules from 15 patients. The 5 radiologists independently reviewed chest CT images at 21 and 45 mAs.

Results: In the phantom study, the Az value for GGO nodules with a CT number of −800 HU was significantly lower at 21 than 180 effective mA (0.86 vs. 0.96; $P < 0.01$). There was no statistically significant difference in the Az value of GGO nodules with a CT number of −650 HU, irrespective of milliamperes used ($P = 0.165$). In the clinical study, 39.5% and 25.8% of GGO were missed at 21 and 45 mAs, respectively.

Conclusions: At MDCT, GGO nodules with a CT number of −650 HU or less were difficult to detect at the lower milliampere settings (21 and 45 mAs).

Key Words: lung cancer screening, ground-glass opacity, detectability, radiation dose, CT number

(*J Comput Assist Tomogr* 2009;33: 49–53)

Low-dose computed tomographic (CT) scanning is a promising method to detect early-stage lung cancer because its detection rate is 2.6- to 10-fold higher than of chest radiography.[1–5] However, low-dose CT screening for lung cancer can return false-negative results. Swensen et al[6] found that nodules were missed in 26% of patients undergoing their first annual CT examination. Nodules with ground-glass opacity (GGO) are more difficult to detect than solid nodules; approximately 70% of lung cancers missed by radiologists at low-dose CT screening were GGO nodules.[7] Although GGO is a nonspecific finding that may be elicited by benign disease such as focal inflammation, focal fibrosis, and adenomatous hyperplasia, it may be attributable to malignant lesions such as bronchioloalveolar carcinoma (BAC) or adenocarcinoma.[7–11] Therefore, the reliable detection of GGO nodules is a critical issue in lung cancer screening with low-dose CT.

To our knowledge, the detectability of GGO nodules by low-dose CT has not been studied quantitatively. Mayo etal[12] reported that a reduced tube current affected the reader evaluation of structures and lung findings on chest CT, suggesting that the radiation dose of CT scans may have implications for the detectability of GGO nodules. On the other hand, because the detectability of lesions on CT scans depends on the attenuation difference between the lesions and the surrounding normal parenchyma,[13] it may be difficult to identify GGO nodules with low attenuation values. In the current study, we investigated the effect of the radiation dose and the attenuation of GGO nodules on their detectability at multidetector CT (MDCT) by using a chest phantom and human subjects.

MATERIALS AND METHODS

Phantom Study

Chest CT Phantom

We used a commercially available chest CT phantom (LSCT001; Kyoto Kagaku Co., Kyoto, Japan) and simulated GGO nodules. The simulated lungs were made of a composite of styrofoam and hard urethane powder in urethane resin adhesive; the simulated tumors were spheres made of acrylic foam and urethane. Details regarding this device have been presented elsewhere.[14] Simulated GGO nodules were placed at 3 levels: the lung apex (upper), tracheal bifurcation (middle), and lung base (lower portion). The CT number of the simulated lung was −900 Hounsfield units (HU). The attenuation of the simulated GGO nodules was −800 HU in the right and −650 HU in the left simulated lung. The diameter of the GGO nodules was 4, 6, 8, 10, and 12 mm in the right and 2, 4, 6, 8, and 10 mm in the left lung. In the observer performance test, we used simulated GGO nodules 6, 8, and 10mm in diameter in both lungs (Fig. 1).

CT Scanning

We used a 40-detector CT scanner (Brilliance-40; Philips Medical Systems, Cleveland, Ohio). The scanning parameters were tube voltage, 120 kVp; detector collimation, 32 × 1.25 mm; beam pitch, 0.719; table speed, 28.76 mm pergantry rotation (gantry rotation time, 0.5 s); acquisition of 5.0-mm

From the *Department of Radiological Sciences, School of Health Sciences; and †Department of Diagnostic Radiology, Graduate School of Medical Sciences, Kumamoto University, Kumamoto, Japan.
Received for publication September 2, 2007; accepted October 12, 2007.
Reprints: Yoshinori Funama, PhD, Department of Radiological Sciences, School of Health Sciences, Kumamoto University, 4-24-1 Kuhonji, Kumamoto 862-0976, Japan (e-mail: funama@kumamoto-u.ac.jp).

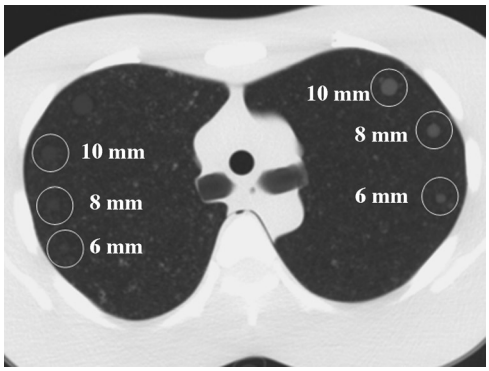

FIGURE 1. Chest phantom. Image of simulated GGO nodules in the middle portion of the right and left lung. In the observer performance test, we placed 6-, 8-, and 10-mm GGO nodules. The CT number of the GGOs and the parenchyma differed by 100 HU in the right and by 250 HU in the left lung.

images reconstructed at 1.0-mm intervals; scan field of view (FOV), 50.0 cm; display FOV, 35.0 cm. Although our CT instrument was a 40-detector CT, the number of the active data acquisition system was 32 at 1.25-mm detector collimation. The effective tube current time products (mAs) were 21, 45, 60, 90, and 180 mAs; these settings were combined with an automatic tube current modulation technique[15] for further radiation-dose reduction. In the scan protocol for focal lung diseases recommended by McGuinness and Naidich,[16] volume CT dose index is approximately 15 mGy; this radiation dose almost corresponds to 180 mAs and 120 kVp on our CT scanner. Therefore, we considered 180 mAs as the standard dose. We decreased the tube current second so as to be 50%, 25%, and 12.5% of 180 mAs. Consequently, the 21 mAs coincided with minimal milliamperes that our CT scanner can allow. Our CT scanner does not allow setting the milliamperes lower than 21 mAs at a pitch of 0.719. In addition, we predicted in advance that tube current second ranging from 45 to 90 mAs might be critical values for detection of GGO nodules. Therefore, we added scan with 60 mAs to the study protocols. The mean and SD of the tube current time products were calculated for all images of each lung portion.

Observer Performance Test for the Detectability of Simulated GGO Nodules

We conducted an observer performance test to investigate the detectability of the simulated GGO nodules. Our institutional review board approved participation of the 5 radiologists. Their prior written informed consent was obtained; their experience ranged from 6 to 18 years (mean ± SD, 9.2 ± 4.5 yrs). The 5 radiologists specialized in body imaging and read chest CT on a regular basis.

For the observer performance test, we extracted 10 × 30-mm rectangular areas that did, or did not, include 1 simulated GGO nodule from images obtained at 21, 45, 60, 90, and 180 mAs. The extracted images were displayed on black-background images. The observers read the extracted images on a color monitor with a spatial resolution of 1200 × 1600 (Radiforce R22; Eizo, Ishikawa, Japan) using a Digital Imaging and Communications in Medicine viewer (Image Vinus Pro, ver. 3.01; Yokogawa Electric Corp., Tokyo, Japan). We prepared 900 extracted images (450 images each from the right and left lung); they consisted of 90 images obtained at each of the 5 different milliampere settings. Each set of 90 images was composed of 30 images obtained at the upper, middle, and lower lung portion; each set of 30 images included 15 images with and 15 without GGO nodules. A window width of 1500 HU and a window level of −600 HU were set asconstants for the visual evaluations.

The readers were blinded to the milliampere setting applied for image acquisition. The time for reading the images was not limited; each reader was allowed to change the window level and width on the monitor screen. A continuous rating scale consisting of a line-marking method was used; each reader expressed the confidence level by placing marks on a 5-cm-long line. To indicate whether an object was presentor not, each reader placed a pencil mark on a bar on the recording forms; definitely present and definitely not present were indicated at the right and left end of the bar, respectively. The images were presented in random order by using a random table.

Clinical Study

Patients

Our study was approved by our institutional review board. Before obtaining their prior written informed consent to undergo CT examinations and to participate in this study, we explained to all patients the purpose of this study, and that their participation did not interfere with any clinical examinations.

Between January and December 2005, we enrolled 15 patients in this study. Inclusion criteria were (1) more than 1 chest CT examination, including high-resolution CT (HRCT) study; and (2) the identification of 1 or more GGO nodules or no abnormal findings on previous HRCT scans. All patients had been originally suspected of having pulmonary nodules on chest radiography in our institute or on CT in another institute and were followed by CT in our institute. Thus, patients included in this study did not undergo CT lung cancer screening. Among the 15 patients, 8 manifested GGO nodules. The patients were 9 women and 6 men; their mean age was 68.0 ± 4.0 years (range, 59–72 yrs). The patients with GGO nodules had between 3 and 8 nodules (mean, 4.8); the total number of GGO nodules in the 8 patients was 38. The CT number of the lung parenchyma ranged from −813 to −911 HU (mean, −889 HU), and the range for the GGO nodules was from −840 to −133 HU (mean, −637 HU). The CT number was equal or less than −800 HU in 5, more than −800 HU and equal or less than −650 HU in 18, and more than −650 HU in 15 GGO nodules (Table 1). Thresholds values of −800 and −650 HU were set to correspond with the phantomstudy. The mean maximum diameter of the GGO nodules was 7.5 mm (range, 3.5–13.9 mm). The size of GGOs in 3 groups categorized by the difference in the CT number of the lung parenchyma and the GGO is shown in Table 1 ($P = 0.163$). Pathological confirmation of the GGO nodules was not obtained in all patients; all patients did not undergo surgery or biopsy. The size of GGO nodules did not change inthe course of this study in all patients.

TABLE 1. Size of GGO Nodules in 3 Groups Categorized by Their CT Number

CT No. the GGO Nodules (HU)	No. GGO Nodules	Mean size (SD), (mm)	Range of Size (mm)	*P*
≤−800	5	6.5 (2.0)	4.0–8.6	
>−800, ≤−650	18	6.2 (1.6)	3.8–8.2	0.163
>−650	15	8.4 (3.1)	4.1–13.9	

TABLE 2. Az Values for the Detection of Simulated GGO Nodules at Each Milliampere

CT No. GGO Nodules (HU)	mAs	Mean Az Value (SD)	*P*
−800	21	0.86 (0.03)	<0.01
	45	0.95 (0.02)	0.78
	60	0.97 (0.02)	0.93
	90	0.97 (0.01)	0.96
	180	0.96 (0.01)	—
−650	21	0.97 (0.01)	1.00
	45	0.98 (0.01)	1.00
	60	0.98 (0.01)	1.00
	90	0.98 (0.01)	1.00
	180	0.98 (0.01)	—

CT Scanning

All patients were scanned with the same CT scanner used in the phantom study (Brilliance-40; Philips Medical Systems). The tube voltage was 120 kVp; detector collimation, 32 × 1.25 mm; reconstruction thickness and interval, 5 mm; beam pitch, 0.719; table speed, 28.76 mm per gantry rotation (gantry rotation time, 0.5 s); acquired 5.0-mm images were reconstructed at 1.0-mm intervals; the scan FOV was 50.0 cm; the display FOV, 35.0 cm; the reconstruction algorithm was lung. The tube current–time product (mAs) was set at 180 mAs (standard dose). We also performed low-dose scans of the whole lungs at 21 and 45 mAs immediately after standard-dose scans. We adopted 2 kinds of milliamperes for low-dose scans because we considered 21 or 45 mAs a critical tube current second for the detection of GGO nodules and because we wanted to minimize the radiation dose in the clinical study. We used the same automatic tube current modulation technique as in the phantom study.

Qualitative Analysis for the Detectability of GGO Nodules

Two chest radiologists with 21 and 12 years of expertise in chest imaging independently reviewed the images obtained at 180 mAs and recorded the presence and location of the GGO nodules. They then decided their presence and location by consensus; this was used as the criterion standard for the further clinical evaluations. They independently measured the maximum diameter of the GGO nodules; the measured values were then averaged for each nodule. We did not conduct observer performance study using receiver operating characteristic (ROC) analysis because it was difficult to confirm the actual presence of individual GGO nodules on clinical images.

The images were displayed using a lung window with acenter of −600 HU and a width of 1500 HU. The 5 radiologists who participated in the observer performance test using the chest phantom also independently reviewed the human chest CT images with the 38 GGO nodules on a color monitor (Radiforce R22, Eizo) using a DICOM viewer (Image Vinus Pro, ver. 3.01); the images were presented in random order. To ensure a blinded evaluation, no information on the milliampere settings was provided. The 5 radiologists recorded the number of GGO nodules and their location in each patient.

Statistical Analysis

We performed ROC analysis[17] to evaluate the detectability of simulated nodules in the phantom study. A binormal ROC curve was fitted to each radiologist's confidence rating data with quasi-maximum likelihood estimation by using the ROCKIT computer program.[18] The area under the best-fit ROC curve plotted in the unit square (Az) was calculated for each fitted curve. We calculated Az values for the right and left lung by averaging the Az values in the upper, middle, and lower phantom lung portion at each of the 5-mAs settings. The Dunnett test was used for multiple comparisons of Az values among the different mAs settings.

In the clinical study, the size of the GGO nodules in 3 groups categorized by their CT number was compared using 1-way analysis of variance.

Differences of $P < 0.05$ were considered statistically significant. Calculation of 1-way analysis of variance and Dunnett test was with a statistical software program (SPSS, version 15.0, Chicago, Ill).

RESULTS

Detectability of GGO Nodules in the Phantom Study

The mean Az value of GGO nodules with a CT number of −800 HU was statistically significantly lower at 21 than at 180 mAs (0.86 vs. 0.96; $P < 0.01$) (Table 2; Figs. 1A, B). On the other hand, there was no statistically significant difference between the mean Az value at 180 mAs and at 45, 60, and 90 mAs. Among nodules with an attenuation of −650HU, there was no statistically significant difference in the mean Az value between GGO nodules scanned at 180 and at 21, 45, 60, and 90 mAs. Figure 2 shows images of the upper portion of the right lung obtained at 21 and 180 mAs.

Detectability of GGO Nodules in the Clinical Study

We found that at 21 mAs, 60% of GGO nodules with a CT number equal to or less than −800 HU were missed; the missed rate dropped to 36.0% at 45 mAs (Table 3). At 21 mAs, 52.2% of GGO nodules with CT number more than 800 HU and equal to or less than −650 HU were missed; the missed rate dropped to 37.8% at 45 mAs. Finally, 17% of GGO nodules with a CT number higher than −650 HU were missed

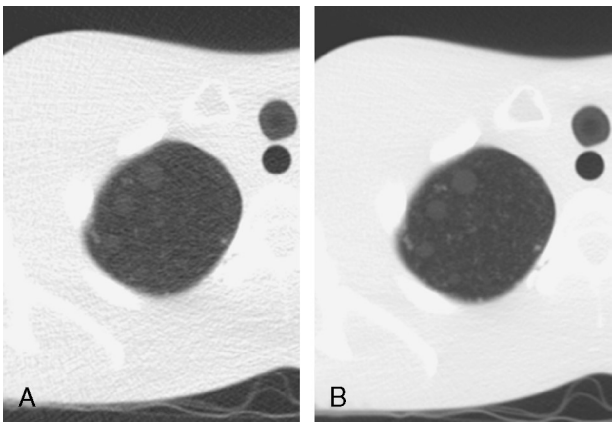

FIGURE 2. Chest phantom. CT images of the upper portion of the right lung. The effective tube current time product (mAs) was 21 (A) and 180 mAs (B).

TABLE 3. Number of GGO Nodules Missed by 5 Radiologists in the Clinical Study

CT No. GGO Nodules (HU)	No. GGO Nodules	mAs	Mean No. GGO Nodules Missed (range)	Percent of GGO Nodules Missed
≤−800	5	21	3.0 (2–5)	60.0
		45	1.8 (1–2)	36.0
>−800, ≤−650	18	21	9.4 (7–13)	52.2
		45	6.8 (3–8)	37.8
>−650	15	21	2.6 (1–5)	17.0
		45	1.2 (0–3)	8.0

at 21 mAs; at 45 mAs, 8.0% of these GGO nodules were missed. Figure 3 shows clinical images obtained at 21, 45, and 180 mAs.

DISCUSSION

Li et al[7] reported that 27 of 85 GGO nodules (31.8%) were missed at annual low-dose CT lung screening examinations. Because they used a single helical CT scanner, a tube current product of 50 or 100 mAs, and a section thickness of 10 mm, it is difficult to compare their results with ours. Nonetheless, a considerable number of GGO nodules may be missed at low-dose CT screening. In our phantom study, the detectability of simulated GGO nodules with a CT number of −800 HU was statistically significantly lower at 21 than at 180 mAs. On the other hand, when the simulated GGO nodules had a CT number of −650 HU, there was no significant difference in the Az value for their detectability at the 5-mAs settings used in this study. Furthermore, in our clinical study, the number of missed GGO nodules at 21 mAs was 1.4 to 2.1 times higher than at 45 mAs, irrespective of their CT number. Our results suggest that scans at 21 mAs orless may be not able to detect GGO nodules with lower CT numbers.

In our clinical study, 36% to 60% of GGO nodules with a CT number of −650 HU or less were missed; the missed rate dropped to 8% to 17% for GGO nodules with CT number higher than −650 HU. Because the size of the GGO nodules in the 3 different groups was not statistically different, we postulate that among GGO nodules of similarsize, the radiologists had difficulty identifying nodules with aCT number of −650 HU or less. On the other hand, in the phantom study, at 21 mAs, the Az value for the detectability of GGO nodules with a CT number of −800 HU or less was statistically significantly lower than at the other milliamperes. In our clinical study, the CT number of missed GGO nodules was higher than expected from the results of our phantom study. On clinical images, the detectability of GGO nodules may be impaired by subtle patient movements or by lung artifacts attributable to various structures. In addition, because the margins of real GGO nodules are frequently ill-defined and their internal texture tends to be in homogeneous, their detection may be more difficult than the identification of GGO nodules on phantom images.

An increase in the image noise may impair the detection of GGO nodules at the minimal tube current second product. In general, the image noise is inversely proportional to the effective tube current. In GGO nodules with a lower CT number, the difference in the CT number between the nodules and the lung parenchyma is relatively small, and an increase in the image noise at the minimal tube current product (21 mAs) may hamper their visualization.

The clinical value of attempting the detection of GGO nodules with CT numbers less than −650 HU may be questioned. Bronchioloalveolar carcinoma often manifest GGO nodules without solid part, and it is often difficult to differentiate BAC from atypical adenomatous hyperplasia (AAH) on CT scans.[19] According to Nomori et al,[10] the mean CT number for AAH and BAC was −697 ± 56 (SD) HU and −541 ± 73 HU, respectively, and the difference between AAH and BAC was statistically significant. Thus, most GGO nodules with a CT number lower than −650 HU may reflect AAH. Although AAH is considered a precursor or even an early-stage lesion of BAC or adenocarcinoma,[20,21] there have been no reports on the progression of AAH to BAC or adenocarcinoma and the detection of GGO nodules whose CT number is lower than −650 HU may be of no clinical significance. However, the natural history of AAH has not been fully elucidated, and a nodular CT number lower than −650 HU does not completely rule out BAC or adenocarcinoma. Furthermore, very faint GGO nodules that have lower CT numbers may represent inflammatory process,for example, healing focal pneumonia. At present, differential diagnosis between inflammatory process showing

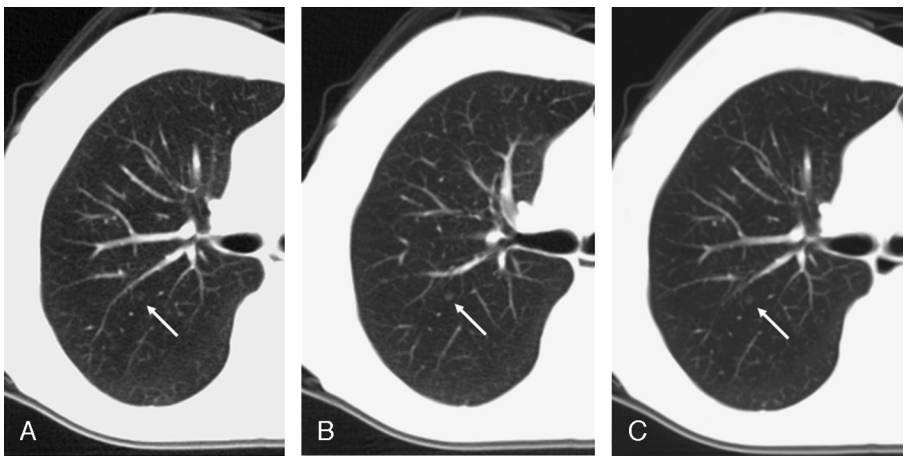

FIGURE 3. Clinical study. Computed tomographic images of the lung of a 59-year-old woman. All images were obtained at the same level. The GGO nodule measured 4.0 mm in diameter (arrow). Low-dose CT images were acquired at 21 (A), 45 (B), and at the standard dose of 180 mAs (C).

focal GGO and BAC by CT has not been established. Therefore, we believe that efforts should be continued to detect GGO nodules with lower CT numbers.

The detection of solid nodules is also important at lung cancer screening with low-dose CT. In our phantom and clinical studies, GGO nodules with higher CT numbers were more easily detected. In general, the larger the difference in the CT number between nodules and surrounding normal parenchyma, the easier is their detection.[13] Because this difference is larger in solid than in GGO nodules, solid nodules may be more easily detected that GGO nodules. Li et al[7] reported that 32% of lung cancers with solid nodules were missed on low-dose CT screens, although most errors were attributable to interpretation, rather than detection error. We postulate that the detection of solid is easier than that of GGO nodules, and quantitative studies to test this hypothesis are under way in our laboratory.

In the near future, lung cancer screens may be performed with thin-section (0.5–1.0 mm) MDCT. Aberle et al[22] proposed a thin-section lung cancer screening MDCT scan protocol because thin-section scans may avoid the partial volume effect and make possible the precise evaluation of pulmonary nodules. However, at low radiation doses, the detection and characterization of GGO nodules may be impaired because on thin-section CT scans, the number of X-ray photons may be reduced and the image noise increased. Therefore, the tube current second product must be optimized at thin-section low-dose CT.

Our results are encumbered by some limitations. First, in the clinical study, we did not obtain pathological confirmation of the GGOs in all patients because some did not undergo surgery. However, 2 chest radiologists independently reviewed HRCT images obtained with 180 mAs and consensually recorded the location of GGOs. Second, in the clinical study, we adopted only 2-mAs levels at low-dose scanning to minimize the patients' radiation exposure. To compensate, in the phantom study, we performed scans at 5different milliampere settings.

In conclusion, GGO nodules with a CT number of 650 HU or less are difficult to detect at MDCT using a lower tube current second product (21 and 45 mAs).

REFERENCES

1. Henschke CI, McCauley DI, Yankelevitz DF, et al. Early lung cancer action project: overall design and findings from baseline screening. *Lancet*. 1999;354:99–105.
2. MacRedmond R, Logan PM, Lee M, et al. Screening for lung cancer using low dose CT scanning. *Thorax*. 2004;59:237–241.
3. Jett JR, Midthun DE. Screening for lung cancer: current status and future directions: Thomas A. Neff lecture. *Chest*. 2004;125:158S–162S.
4. Diederich S, Thomas M, Semik M, et al. Screening for early lung cancer with low-dose spiral computed tomography: results of annual follow-up examinations in asymptomatic smokers. *Eur Radiol*. 2004;14:691–702.
5. Miettinen OS, Henschke CI. CT screening for lung cancer: coping with nihilistic recommendations. *Radiology*. 2001;221:592–596; discussion 597.
6. Swensen SJ, Jett JR, Sloan JA, et al. Screening for lung cancer with low-dose spiral computed tomography. *Am J Respir Crit Care Med*. 2002;165:508–513.
7. Li F, Sone S, Abe H, et al. Lung cancers missed at low-dose helical CT screening in a general population: comparison of clinical, histopathologic, and imaging findings. *Radiology*. 2002;225:673–683.
8. Li F, Sone S, Abe H, et al. Malignant versus benign nodules at CT screening for lung cancer: comparison of thin-section CT findings. *Radiology*. 2004;233:793–798.
9. Kodama K, Higashiyama M, Yokouchi H, et al. Natural history of pure ground-glass opacity after long-term follow-up of more than 2 years. *Ann Thorac Surg*. 2002;73:386–392; discussion 392–383.
10. Nomori H, Ohtsuka T, Naruke T, et al. Differentiating between atypical adenomatous hyperplasia and bronchioloalveolar carcinoma using the computed tomography number histogram. *Ann Thorac Surg*. 2003;76:867–871.
11. Kakinuma R, Ohmatsu H, Kaneko M, et al. Progression of focal pure ground-glass opacity detected by low-dose helical computed tomography screening for lung cancer. *J Comput Assist Tomogr*. 2004;28:17–23.
12. Mayo JR, Kim KI, MacDonald SL, et al. Reduced radiation dose helical chest CT: effect on reader evaluation of structures and lung findings. *Radiology*. 2004;232:749–756.
13. Baron RL. Understanding and optimizing use of contrast material for CT of the liver. *AJR Am J Roentgenol*. 1994;163:323–331.
14. Muramatsu Y, Tsuda Y, Nakamura Y, et al. The development and use of a chest phantom for optimizing scanning techniques on a variety of low-dose helical computed tomography devices. *J Comput Assist Tomogr*. 2003;27:364–374.
15. Kalra MK, Maher MM, Toth TL, et al. Comparison of Z-axis automatic tube current modulation technique with fixed tube current CT scanning of abdomen and pelvis. *Radiology*. 2004;232:347–353.
16. McGuinness G, Naidich DP. Multislice computed tomography of the chest. In: Silverman P, ed. *Multislice Computed Tomography: A Practical Approach to Clinical Protocol*. Philadelphia, PA: Lippincott Williams & Wilkins; 2002:161.
17. Obuchowski NA. Receiver operating characteristic curves and their use in radiology. *Radiology*. 2003;229:3–8.
18. Metz CE, Herman BA, Shen JH. Maximum likelihood estimation of receiver operating characteristic (ROC) curves from continuously-distributed data. *Stat Med*. 1998;17:1033–1053.
19. Henschke CI, Yankelevitz DF, Mirtcheva R, et al. CT screening for lung cancer: frequency and significance of part-solid and nonsolid nodules. *AJR Am J Roentgenol*. 2002;178:1053–1057.
20. Kitamura H, Kameda Y, Ito T, et al. Atypical adenomatous hyperplasia of the lung. Implications for the pathogenesis of peripheral lung adenocarcinoma. *Am J Clin Pathol*. 1999;111:610–622.
21. Noguchi M, Morikawa A, Kawasaki M, et al. Small adenocarcinoma of the lung. Histologic characteristics and prognosis. *Cancer*. 1995;75:2844–2852.
22. Aberle DR, Gamsu G, Henschke CI, et al. A consensus statement of the Society of Thoracic Radiology: screening for lung cancer with helical computed tomography. *J Thorac Imaging*. 2001;16:65–68.